Available online at www.sciencedirect.com
SCIENCE DIRECT
Journal of Organometallic Chemistry 691 (2006) 1845–1856
Journal of Organometallic Chemistry
www.elsevier.com/locate/jorganchem

A quest for triplet silylenes $XHSi_3$ at ab initio and DFT levels (X = H, F, Cl and Br)

M.Z. Kassaee *, S.M. Musavi, M. Ghambarian

Department of Chemistry, Tarbiat Modarres University, P.O. Box 14155-4838, Tehran, Iran

Received 24 October 2005; received in revised form 9 December 2005; accepted 12 December 2005
Available online 20 February 2006

Abstract

Four ground state triplet silylenes are found among 30 possible silylenic $XHSi_3$ structures (X = H, F, Cl and Br), at seven ab initio and DFT levels including: B3LYP/6-311++G**, HF/6-311++G**, MP3/6-311G*, MP2/6-311+G**, MP4(SDTQ)/6-311++G**, QCISD(T)/6-311++G** and CCSD(T)/6-311++G**. The latter six methods indicate that the triplet states of 3-flouro-1,2,3-trisilapropadienylidene, 1-chloro-1,2,3-trisilapropargylene and 3-chloro-1,2,3-trisilapropargylene are energy minima. These triplets appear more stable than their corresponding singlet states which cannot even exist for showing negative force constants. Also, triplet state of 1-flouro-1,2,3-trisilapropargylene is possibly accessible for being an energy minimum, since its corresponding singlet state is not a real isomer. Some discrepancies are observed between energetic and/or structural results of DFT vs. ab initio data.

Keywords: Silylene; H_2Si_3; $FHSi_3$; $ClHSi_3$; $BrHSi_3$; 3-Flouro-1,2,3-trisilapropadienylidene; 1-Chloro-1,2,3-trisilapropargylene; 3-Chloro-1,2,3-trisilapropargylene; 1-Flouro-1,2,3-trisilapropargylene; Ab initio; DFT

1. Introduction

Recently much attention has been directed to the question of singlet/triplet energy gaps, in the heavier carbene analogues consisting of: silylenes [1], germylenes [2], stannylenes and plumbylenes [3]. Quantum chemical calculations on several silylenes and germylenes have shown their ground states to be mostly singlet, in contrast to carbenes, where the triplet is of lower energy [4,5]. Both electronic and steric effects might affect singlet–triplet energy separations (ΔE_{t-s}) [6]. The lowest electronic states of methyl-, silyl-, and lithium-substituted silylenes have been investigated. Methyl group acts like halogens. It increases the singlet–triplet energy splittings of group 14 divalent species. SiH_3 behaves as an electropositive substituent and decreases this energy gap. When it gets to the more electropositive lithium-substituted silylenes, the ground state switches from singlet to the triplet state. The effects of the electropositive substituents on ΔE_{t-s} prevail against those of the electronegative ones [7–9].

To understand the molecules scrutinized in this work, we take up the properties of multiple-bonds. In a multiple-bond, made from the second row elements, the bond length is inversely proportional to the corresponding bond order. Such is not usually the case for the multiple-bonds, made from the third period onward. They often have long bond distances and low π-bond energies, which may be due to the poor overlap of their p-orbitals, that makes their corresponding molecules extremely unstable [10,11]. However, evidence confirming that these compounds exist in cryogenic matrix or gas phase, as short-lived species, has accumulated from studies arising from the latter half of the 1960s to the 1970s. Stable compounds having P=C bonds [12], as well as Si=C [13], Si=Si [14], and P=P [15] have been synthesized and isolated for the first time in 1978 and 1981, respectively. Consequently, attention has expanded to silicon–silicon double bonds and triple bonds containing silicon [16–18], as well as the small silicon-containing rings [19]. More recently, Kira et al. reported

* Corresponding author. Tel.: +98 912 1000392; fax: +98 21 8006544.
E-mail address: Kassaeem@Modares.ac.ir (M.Z. Kassaee).

0022-328X/$ - see front matter © 2006 Published by Elsevier B.V.
doi:10.1016/j.jorganchem.2005.12.045

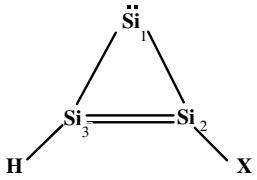

2-X-1,2,3-trisilacyclopropenylidene
(singlet $\mathbf{1}_{s\text{-}X}$; triplet, $\mathbf{1}_{t\text{-}X}$)

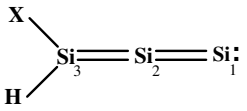

3-X-1,2,3-trisilapropadienylidene
(singlet $\mathbf{2}_{s\text{-}X}$; triplet $\mathbf{2}_{t\text{-}X}$)

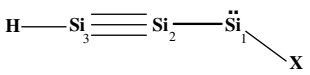

1-X-1,2,3- trisilapropargylene
(singlet $\mathbf{3}_{s\text{-}X}$; triplet $\mathbf{3}_{t\text{-}X}$)

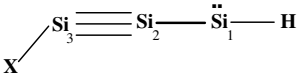

3-X-1,2,3-trisilapropargylene
(singlet $\mathbf{4}_{s\text{-}X}$; triplet $\mathbf{4}_{t\text{-}X}$)

Fig. 1. The four structures considered for singlet (**s**) and/or triplet (**t**) states of silylenic $XHSi_3$ (where X = H, F, Cl and Br).

interesting examples of cyclic disilenes [20], spiropentasiladiene [21], 4-silatriafulvene [22], a silicon-containing fused bicyclic compound with a highly strained bridgehead double bond [23], and a disilane with a long Si–Si bridge [24]. Also, a stable silicon analogue of an allene, with a core of Si=Si=Si unit, with sp-hybridized silicon atoms, was synthesized [25]. Unlike its linear carbon counterpart, trisilaallene is 'bent', but the compound is relatively stable. Finally, the synthesis and characterization of the first disilyne with a Si≡Si triple-bond is reported by Sekiguchi and coworkers [26]. The structure and bonding of Si compounds are inherently complex. The well established bonding rules of carbon chemistry are of little help in deducing the compounds of Si and the other heavier group 14 analogues [27].

Following up on our studies on divalent species of group 14 elements [3,28–34], as well as the specific studies of Maier et al. on the small and matrix isolable silylenes C_2HXSi [35]; a quest is made for triplet silylenes $XHSi_3$ at ab initio and DFT levels (X = H, F, Cl and Br) (see Fig. 1).

2. Computational methods

Full geometrical optimizations are performed on singlet and triplet H_2Si_3 silylenes, as well as their halogen substituted analogues consisting of $FHSi_3$, $ClHSi_3$ and $BrHSi_3$, each with four skeletal arrangements containing: 2-X-1,2,3-trisilacyclopropenylidene (**1**), 3-X-1,2,3-trisilapropadienylidene (**2**), 1-X-1,2,3-trisilapropargylene (**3**), and 3-X-1,2,3-trisilapropargylene (**4**), at the HF, DFT, the second and third-order MØller–Plesset (MP2, MP3) methods, where X = H, F, Cl and Br (Fig. 1). All optimizations are performed with no imposed constraints, making the starting structures free to transform through optimizations. For Hartree–Fock (HF) calculations, the 6-311++G** basis set is employed. Likewise, for DFT calculations the, Becke's hybrid three-parameter functional combined with the Lee–Yang–Parr non-local correlation functional B3LYP [36] with the 6-311++G** basis set is employed. For MP2, 6-311+G** and MP3, the 6-311G* basis sets is used. The MP2/6-311+G** optimized geometries are submitted as input for single-point calculations at the fourth-order MP (MP4), QCISD(T) [37–39] and CCSD(T) levels [40] with the 6-311++G** basis set. Singlet states are

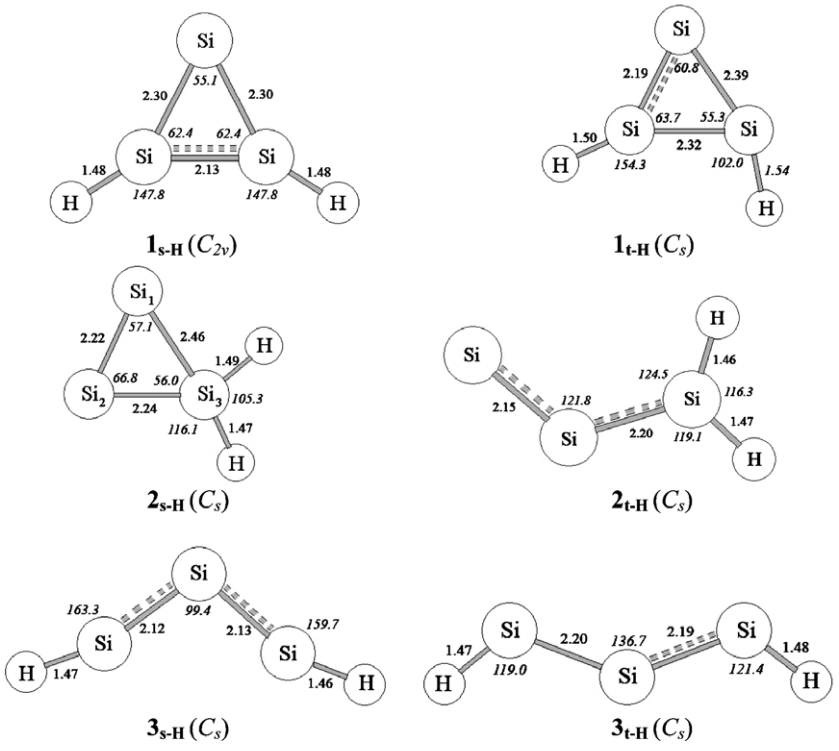

Fig. 2. MP2/6-311+G** optimized geometries and point groups of six silylenic H_2Si_3 structures, with bond lengths given in angstroms (Å) and bond angles in degrees (°).

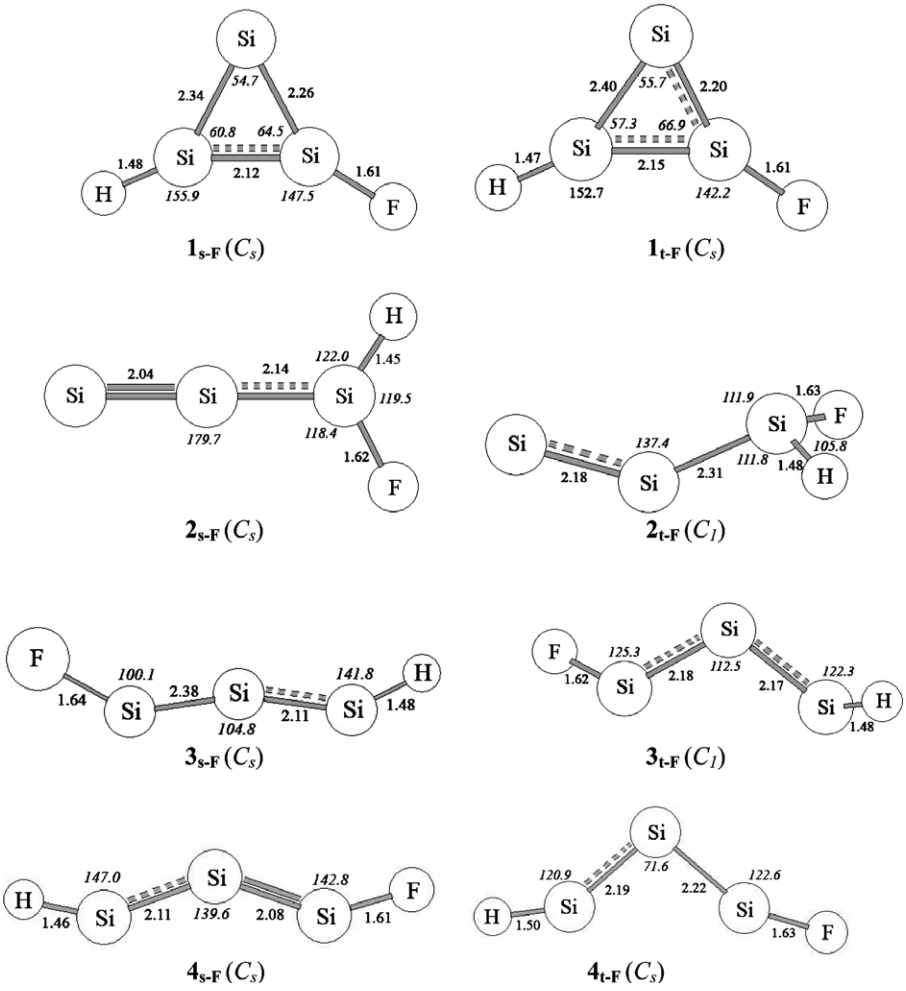

Fig. 3. MP2/6-311+G** optimized geometries and point groups for eight fluorosilylenic $FHSi_3$ structures, with bond lengths given in angstroms (Å) and bond angles in degrees (°).

calculated with spin-restricted wave functions. The spin projected wave functions are employed for triplet states. This is to predict the singlet–triplet energy differences more reliably. Atomic charges and energies of the HOMO and LUMO orbitals are obtained via NBO analysis [41]. The harmonic vibrational frequencies and zero point energies (ZPE) of these species are calculated for each optimized structure at HF and DFT levels. The vibrational frequencies and ZPE data at the HF/6-311++G** and B3LYP/6-311++G** are scaled by 0.89 and 0.98, respectively [42,43]. This is to account for the difference between the harmonic and anharmonic oscillations of the actual bonds. For minimum state structures, only real frequency values and for the transition states, only a single imaginary frequency value is accepted. All calculations, in this paper are performed using the GAUSSIAN 98 package [44].

3. Results and discussion

Ab initio comparisons are carried out among isomeric sets of singlet (**s**) and triplet (**t**) silylenes $XHSi_3$, for X = H, F, Cl and Br, confined to four possible structures: 2-X-1,2,3-trisilacyclopropenylidene ($\mathbf{1_{s\text{-}X}}$ and/or $\mathbf{1_{t\text{-}X}}$); 3-X-1,2,3-trisilapropadienylidene ($\mathbf{2_{s\text{-}X}}$ and/or $\mathbf{2_{t\text{-}X}}$); 1-X-1,2,3-trisilapropargylene ($\mathbf{3_{s\text{-}X}}$ and/or $\mathbf{3_{t\text{-}X}}$); and 3-X-1,2,3-trisilapropargylene ($\mathbf{4_{s\text{-}X}}$ and/or $\mathbf{4_{t\text{-}X}}$) (Fig. 1). Relative energies of these 30 structures are calculated and sorted into four tables, with respect to the substituent (X) employed, using HF, B3LYP, MP2, MP3, MP4(SDTQ), QCISD(T) and CCSD(T) methods with 6-311G*, 6-311+G** and 6-311++G** basis sets (X = H, Table 1; X = F, Table 2; X = Cl, Table 3; and X = Br, Table 4). To reach accessible triplet ground states of $XHSi_3$ silylenes, force constant calculations were carried out, where 17 out of 30 structures appeared as transition states. From the remaining 13 minima, triplet states of $\mathbf{2_{t\text{-}F}}$, $\mathbf{3_{t\text{-}Cl}}$ and $\mathbf{4_{t\text{-}Cl}}$ showed higher stability than their corresponding singlet states. Moreover, $\mathbf{3_{t\text{-}F}}$ is a minimum which appears not to have a real singlet state. Energetic results are very dependent on the computational methods employed. This is not surprising since the silylenic species studied are electron-deficient and there could be low-lying unoccupied orbitals which make the SCF calculations give different solutions

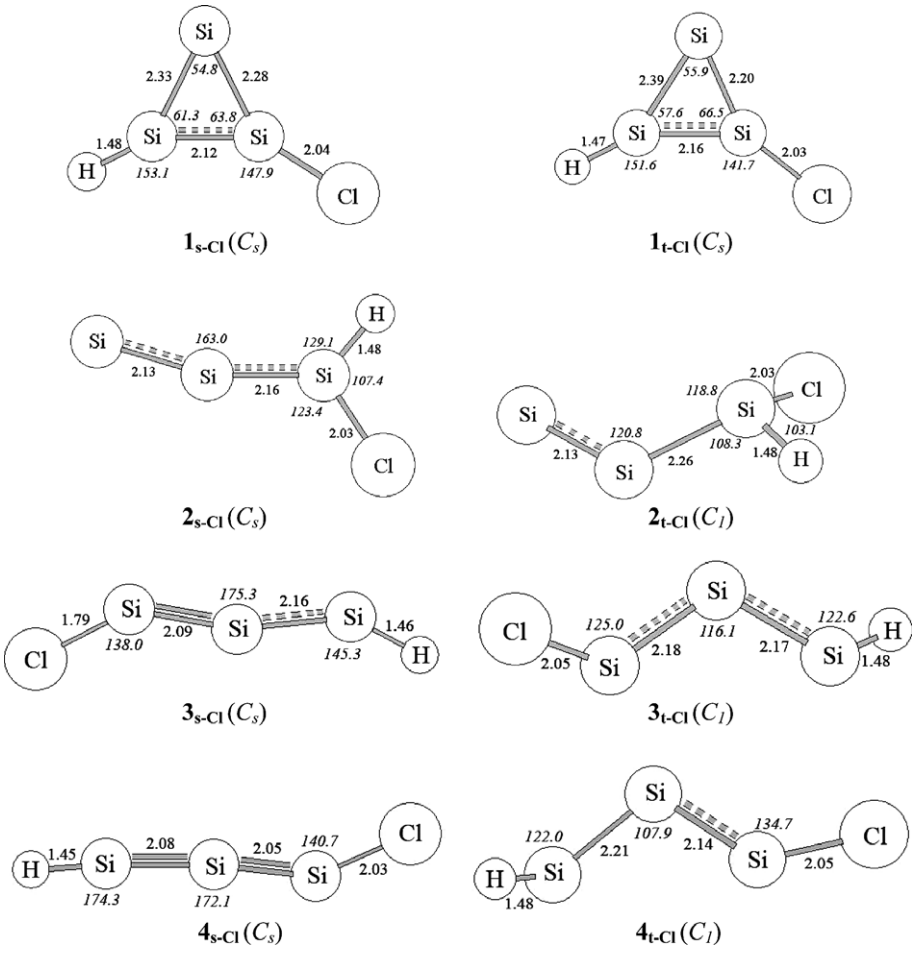

Fig. 4. MP2/6-311+G** optimized geometries and point groups for eight chlorosilylenic $ClHSi_3$ structures, with bond lengths given in angstroms (Å) and bond angles in degrees (°).

[45]. Moreover, the energy results obtained at HF level are very remote from those obtained through other calculation methods. Nevertheless, a rather manifest consistency prevails between the calculated relative energy trends (Tables 1–4). The magnitudes of relative energies calculated at B3LYP are lower than the other six employed calculation methods (Tables 1–4). The relative energies, calculated at QCISD(T) and CCSD(T) levels, are quite similar to each other, while they appear somewhat different from those of MP4. These differences are more pronounced for triplet species, possibly due to the spin-contamination problem expected for MP4 calculations [46,47]. Hence, in the reminder of our discussion the high level CCSD(T) single-point energy results are preferred over other calculation methods. In cases of $\mathbf{2_{s\text{-}F}}$, $\mathbf{2_{t\text{-}F}}$, $\mathbf{3_{s\text{-}F}}$ and $\mathbf{2_{t\text{-}Cl}}$, where single-point energy results are not provided, the MP2 results are reported. Even though B3LYP appears reliable for computing geometrical parameters, in this study some discrepancy is observed between B3LYP geometrical parameter vs. those obtained from the six ab initio methods employed [32,45,47]. For example, the optimized structure of $\mathbf{4_{t\text{-}Cl}}$ is cyclic at B3LYP, while it is acyclic at MP2. Hence, MP2/6-311+G** optimized geometrical parameters of these 30 structures are calculated and divided into four figures, with respect to the substituent (X) employed (X = H, Fig. 2; X = F, Fig. 3; X = Cl, Fig. 4; and X = Br, Fig. 5). In general, the optimized structures of silylenic species **1**–**4**, differ with the original inputs (Figs. 2–5). Moreover, the singlet acyclic $\mathbf{2_{s\text{-}H}}$ structure modify to a cyclic structure. The accessibility of such five-coordinated silicon or H-bridged structures is expected in the chemistry of silicon compounds [27]. The energies of HOMO and LUMO orbitals are attained through NBO analyses for both singlet and triplet structures of $XHSi_3$. Rather linear correlations are found between the LUMO–HOMO energy gaps of singlet $XHSi_3$ silylenes $\mathbf{2_{s\text{-}X}}$ and/or $\mathbf{4_{s\text{-}X}}$ and their corresponding singlet–triplet energy separations, $\Delta E_{s-t,X}$, for X = H, F, Cl and Br (Fig. 6). The decreasing trend of LUMO–HOMO energy gaps as a function of X, for $\mathbf{2_{s\text{-}X}}$ follows electropositivity: Br > Cl > F. The linearity trend is: $\mathbf{4_{s\text{-}X}}(R^2 = 0.66) > \mathbf{2_{s\text{-}X}}(R^2 = 0.6)$, where R^2 = correlation coefficient. One of the significant parameters affecting the $\Delta E_{s\text{-}t}$, is the magnitude of divalent bond angle [32]. Bending potential energy curves for divalent $\mathbf{3_{s\text{-}H}}$ and $\mathbf{3_{t\text{-}H}}$ structures are calculated at MP2/6-311+G**

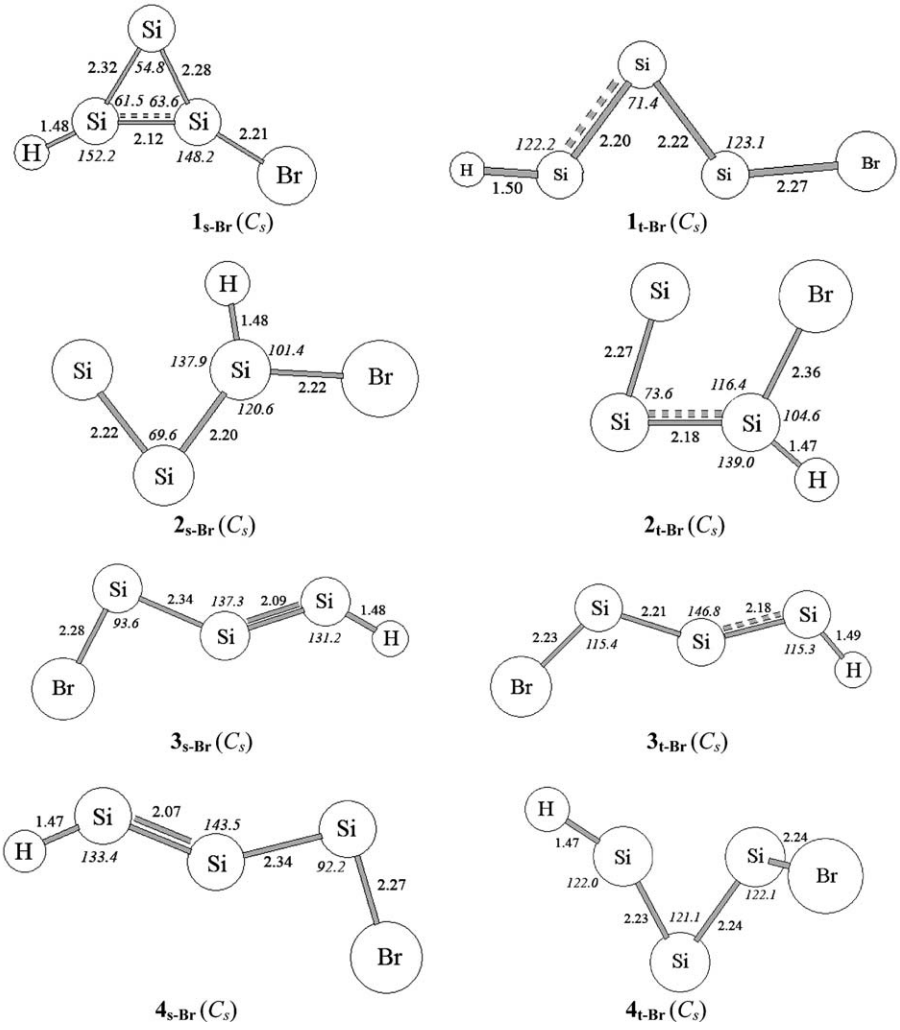

Fig. 5. MP2/6-311+G** optimized geometries and point groups for eight bromosilylenic $BrHSi_3$ structures, with bond lengths given in angstroms (Å) and bond angles in degrees (°).

(Fig. 7). The singlet state $\mathbf{3_{s\text{-}H}}$ and triplet state $\mathbf{3_{t\text{-}H}}$ cross at the $\angle HSi_1Si_2$ divalent angle about 125°.

To save space, calculated harmonic frequencies of $XHSi_3$ species are not included in the paper, but are available upon request. B3LYP/6-311++G** as well as HF/6-311++G** force constant calculations show that the 17 species $\mathbf{1_{t\text{-}H}}$, $\mathbf{1_{t\text{-}F}}$, $\mathbf{1_{t\text{-}Cl}}$, $\mathbf{1_{t\text{-}Br}}$, $\mathbf{2_{s\text{-}F}}$, $\mathbf{2_{t\text{-}H}}$, $\mathbf{2_{t\text{-}Br}}$, $\mathbf{3_{s\text{-}H}}$, $\mathbf{3_{s\text{-}F}}$, $\mathbf{3_{s\text{-}Cl}}$, $\mathbf{3_{s\text{-}Br}}$, $\mathbf{3_{t\text{-}H}}$, $\mathbf{3_{t\text{-}Br}}$, $\mathbf{4_{s\text{-}F}}$, $\mathbf{4_{t\text{-}F}}$, $\mathbf{4_{s\text{-}Cl}}$ and $\mathbf{4_{s\text{-}B}}$ have at least one imaginary frequency and exist as transition states on their corresponding potential energy surfaces (Tables 1–4). The NBO atomic charges are calculated for singlet (**s**) and triplet (**t**) states of $XHSi_3$ species (Tables 5 and 6). Finally, the NBO hybridizations for singlet (**s**) and triplet (**t**) states of cyclic $\mathbf{1_{s\text{-}X}}$ and $\mathbf{1_{t\text{-}X}}$ structures are calculated (Table 7).

3.1. Cyclic vs. acyclic silylenes

All singlet cyclic 2-X-1,2,3-trisilacyclopropenylidenes, $\mathbf{1_{s\text{-}X}}$, appear more stable than their corresponding triplet states, $\mathbf{1_{t\text{-}X}}$ (Fig. 1, Tables 1–4). This is due to the angle-strains involved in $\mathbf{1_{t\text{-}X}}$ and the aromatic character associated with $\mathbf{1_{s\text{-}X}}$ species. These results are consistent with those described for singlet and triplet states of analogues carbenic C_3HX, C_2HNX as well as silylenic C_2H_2Si and CHNSi structures [8,32–35]. The cyclic $XHSi_3$, with either singlet or triplet electronic states, maintain their input structures more readily through optimizations than the acyclic structures (except for $\mathbf{1_{t\text{-}Br}}$ which undergoes a Si=Si bond cleavage to form an acyclic structure) (Figs. 2–5). Apparently, the aromatic character, the large size of Si atoms, and/or the longer Si–Si bonds reduce the strain in these cyclic structures [20]. This is in contrast to the analogous, highly energetic, cyclic triplet carbenic C_3HX, and/or the silylenic C_2HXSi species, where the originally adopted cyclic structures may even rupture during the optimizations [29,32]. Interestingly the minimum $\mathbf{1_{s\text{-}H}}$ has a C_{2v} point group, while all the other cyclic species have merely a plane of symmetry with a C_s point group (Figs. 2–5 and Table 5). The orientation of hydrogen atoms around Si_2=Si_3 double bond in $\mathbf{1_{t\text{-}H}}$ is nearly "*cis*-bent". Variations of the $\angle Si_2Si_1Si_3$ divalent angle of singlet $\mathbf{1_{s\text{-}X}}$ as a function of

Table 1
Relative energies (kcal/mol) of H_2Si_3 structures which include singlet states of 2-X-1,2,3-trisilacyclopropenylidene ($\mathbf{1_{s\text{-}H}}$), 3-X-1,2,3-trisilapropadienylidene ($\mathbf{2_{s\text{-}H}}$) and 1-X-1,2,3-trisilapropargylene ($\mathbf{3_{s\text{-}H}}$) as well as their corresponding triplet states $\mathbf{1_{t\text{-}H}}$, $\mathbf{2_{t\text{-}H}}$ and $\mathbf{3_{t\text{-}H}}$, calculated at seven levels of theory; along with number of imaginary frequencies (NIM), ZPE corrections, dipole moments (Debye) at MP2/6-311+G** and vibrational zero point energies (VZPE/kcal/mol) at B3LYP/6-311++G** are included

Structure	Relative energies (kcal/mol)							(NIM)	Dipole moments (D)	VZPE (kcal/mol)
	[a]HF/6-311++G**	[a]MP2/6-311+G**	[a]MP3/6-311G*	B3LYP/6-311++G**	[a]MP4(SDTQ)/6-311++G**	[a]QCISD(T)/6-311++G**	[a]CCSD(T)/6-311++G**	B3LYP/6-311++G**	MP2/6-311+G**	B3LYP/6-311++G**
[b]$\mathbf{1_{s\text{-}H}}$	[1]0.00	[2]0.00	[3]0.00	[4]0.00	[5]0.00	[6]0.00	[7]0.00	0	1.69	10.77
$\mathbf{1_{t\text{-}H}}$	19.14	54.41	47.68	45.61	53.99	53.02	53.13	2	0.83	9.08
$\mathbf{2_{s\text{-}H}}$	28.78	5.38	5.59	5.85	4.53	5.06	5.07	0	0.49	10.63
$\mathbf{2_{t\text{-}H}}$	27.59	64.88	45.26	34.55	46.76	38.33	38.71	1	0.26	9.82
$\mathbf{3_{s\text{-}H}}$	99.11	97.26	134.07	23.59	93.50	90.02	90.21	1	0.73	9.24
$\mathbf{3_{t\text{-}H}}$	55.99	58.08	57.87	45.71	57.61	45.73	46.01	1	0.40	9.26

[a] ZPE not included.
[b] The lowest energy minimum is set at 0.00 kcal/mol; the original total energies (hartrees) corresponding to the lowest energy minimum $\mathbf{1_{s\text{-}H}}$ at various levels of theory: (1) −867.859104, (2) −868.1242164, (3) −868.1271315, (4) −869.6569117, (5) −868.174464, (6) −868.1768386, (7) −868.1763972.

Table 2
Relative energies (kcal/mol) of $FHSi_3$ structures which include singlet states of 2-X-1,2,3-trisilacyclopropenylidene ($\mathbf{1_{s\text{-}F}}$), 3-X-1,2,3-trisilapropadienylidene ($\mathbf{2_{s\text{-}F}}$), 1-X-1,2,3-trisilapropargylene ($\mathbf{3_{s\text{-}F}}$) and 3-X-1, 2, 3-trisilapropargylene ($\mathbf{4_{s\text{-}F}}$), as well as their corresponding triplet states $\mathbf{1_{t\text{-}F}}$, $\mathbf{2_{t\text{-}F}}$, $\mathbf{3_{t\text{-}F}}$ and $\mathbf{4_{s\text{-}F}}$ calculated at seven levels of theory; along with number of imaginary frequencies (NIM), ZPE corrections, dipole moments (Debye) at MP2/6-311 + G** and vibrational zero point energies (VZPE/kcal/mol) at B3LYP/6-311 + +G** are included

Structure	Relative energies (kcal/mol)							(NIM)	Dipole moments (D)	VZPE (kcal/mol)
	[a]HF/6-311++G**	[a]MP2/6-311+G**	[a]MP3/6-311G*	B3LYP/6-311++G**	[a]MP4(SDTQ)/6-311++G**	[a]QCISD(T)/6-311++G**	[a]CCSD(T)/6-311++G**	B3LYP/6-311++G**	MP2/6-311+G**	B3LYP/6-311++G**
[b]$\mathbf{1_{s\text{-}F}}$	[1]0.00	[2]0.00	[3]0.00	[4]0.00	[5]0.00	[6]0.00	[7]0.00	0	2.04	7.97
$\mathbf{1_{t\text{-}F}}$	33.16	52.23	108.94	45.47	65.46	63.35	63.72	1	1.37	7.00
$\mathbf{2_{s\text{-}F}}$	184.51	178.50	246.67	5.75	162.60	–	–	1	3.45	8.08
$\mathbf{2_{t\text{-}F}}$	22.96	44.96	46.68	30.38	60.50	–	–	0	1.65	7.59
$\mathbf{3_{s\text{-}F}}$	111.14	24.77	72.82	21.89	–	–	–	1	2.51	6.84
$\mathbf{3_{t\text{-}F}}$	19.41	59.96	129.80	34.10	59.00	43.60	43.61	0	2.07	6.59
$\mathbf{4_{s\text{-}F}}$	110.70	116.75	186.82	23.16	111.28	93.94	85.39	1	2.16	6.95
$\mathbf{4_{t\text{-}F}}$	18.27	31.91	133.03	26.62	76.03	63.45	63.74	1	1.91	7.19

[a] ZPE not included.
[b] The lowest energy minimum is set at 0.00 kcal/mol; the original total energies (hartrees) corresponding to the lowest energy minimum $\mathbf{1_{s\text{-}F}}$ at various levels of theory: (1) −966.8006539, (2) −967.2680601, (3) −967.2620185, (4) −968.9867126, (5) −967.318776, (6) −967.3183991, (7) −967.3174319.

Table 3
Relative energies (kcal/mol) of $ClHSi_3$ structures which include singlet states of 2-X-1,2,3-trisilacyclopropenylidene ($\mathbf{1}_{s\text{-}Cl}$), 3-X-1,2,3-trisilapropadienylidene ($\mathbf{2}_{s\text{-}Cl}$), 1-X-1,2,3-trisilapropargylene ($\mathbf{3}_{s\text{-}Cl}$) and 3-X-1,2,3-trisilapropargylene ($\mathbf{4}_{s\text{-}Cl}$), as well as their corresponding triplet states $\mathbf{1}_{t\text{-}Cl}$, $\mathbf{2}_{t\text{-}Cl}$, $\mathbf{3}_{t\text{-}Cl}$ and $\mathbf{4}_{s\text{-}Cl}$ calculated at seven levels of theory; along with number of imaginary frequencies (NIM), ZPE corrections, dipole moments (Debye) at MP2/6-311+G** and vibrational zero point energies (VZPE/kcal/mol) at B3LYP/6-311++G** are included

Structure	Relative energies (kcal/mol)							(NIM)	Dipole moments (D)	VZPE (kcal/mol)
	[a]HF/ 6-311++G**	[a]MP2/ 6-311+G**	[a]MP3/ 6-311G*	B3LYP/ 6-311++G**	[a]MP4(SDTQ)/ 6-311++G**	[a]QCISD(T)/ 6-311++G**	[a]CCSD(T)/ 6-311++G**	B3LYP/ 6-311++G**	MP2/ 6-311+G**	B3LYP/ 6-311++G**
[b]$\mathbf{1}_{s\text{-}Cl}$	[1]0.00	[2]0.00	[3]0.00	[4]0.00	[5]0.00	[6]0.00	[7]0.00	0	1.84	7.37
$\mathbf{1}_{t\text{-}Cl}$	32.95	53.07	93.33	45.71	52.51	46.50	46.74	1	0.99	6.37
$\mathbf{2}_{s\text{-}Cl}$	32.19	28.96	–	7.00	107.98	102.31	102.11	0	1.82	7.45
$\mathbf{2}_{t\text{-}Cl}$	18.31	60.29	44.98	30.32	48.07	–	–	0	1.67	7.03
$\mathbf{3}_{s\text{-}Cl}$	137.57	139.85	117.93	22.57	110.36	103.71	102.17	1	0.87	6.26
$\mathbf{3}_{t\text{-}Cl}$	16.97	58.80	111.84	34.23	57.81	42.88	42.95	0	2.01	6.11
$\mathbf{4}_{s\text{-}Cl}$	121.69	124.73	159.32	22.57	119.71	107.84	103.58	1	2.10	6.26
$\mathbf{4}_{t\text{-}Cl}$	16.97	61.01	111.84	20.88	59.98	45.29	45.44	0	1.87	6.77

[a] ZPE not included.
[b] The lowest energy minimum is set at 0.00 kcal/mol; the original total energies (hartrees) corresponding to the lowest energy minimum $\mathbf{1}_{s\text{-}Cl}$ at various levels of theory: (1) −1326.83728, (2) −1327.231099, (3) −1327.24683, (4) −1329.3332, (5) −1327.290851, (6) −1327.29269, (7) −1327.292051.

Table 4
Relative energies (kcal/mol) of $BrHSi_3$ structures which include singlet states of 2-X-1,2,3-trisilacyclopropenylidene ($\mathbf{1}_{s\text{-}Br}$), 3-X-1,2,3-trisilapropadienylidene ($\mathbf{2}_{s\text{-}Br}$), 1-X-1,2,3-trisilapropargylene ($\mathbf{3}_{s\text{-}Br}$) and 3-X-1, 2, 3-trisilapropargylene ($\mathbf{4}_{s\text{-}Br}$), as well as their corresponding triplet states $\mathbf{1}_{t\text{-}Br}$, $\mathbf{2}_{t\text{-}Br}$, $\mathbf{3}_{t\text{-}Br}$ and $\mathbf{4}_{s\text{-}Br}$ calculated at seven levels of theory; along with number of imaginary frequencies (NIM), ZPE corrections, dipole moments (Debye) at MP2/6-311+G** and vibrational zero point energies (VZPE/kcal/mol) at B3LYP/6-311++G** are included

Structure	Relative energies (kcal/mol)							(NIM)	Dipole moments (D)	VZPE (kcal/mol)
	[a]HF/ 6-311++G**	[a]MP2/ 6-311+G**	[a]MP3/ 6-311G*	B3LYP/ 6-311++G**	[a]MP4(SDTQ)/ 6-311++G**	[a]QCISD(T)/ 6-311++G**	[a]CCSD(T)/ 6-311++G**	B3LYP/ 6-311++G**	MP2/ 6-311+G**	B3LYP/ 6-311++G**
[b]$\mathbf{1}_{s\text{-}Br}$	[1]0.00	[2]0.00	[3]–	[4]0.00	[5]0.00	[6]0.00	[7]0.00	0	1.78	7.15
$\mathbf{1}_{t\text{-}Br}$	41.86	33.34	–	27.87	34.44	30.19	30.48	1	2.25	6.37
$\mathbf{2}_{s\text{-}Br}$	10.64	6.96	–	4.49	6.16	6.49	6.54	0	1.54	7.16
$\mathbf{2}_{t\text{-}Br}$	21.44	50.60	–	39.42	48.99	43.55	43.78	1	0.91	6.46
$\mathbf{3}_{s\text{-}Br}$	26.20	31.48	–	22.38	26.17	23.72	24.09	1	1.71	6.05
$\mathbf{3}_{t\text{-}Br}$	36.54	–	–	27.87	63.39	50.59	50.86	1	1.98	6.37
$\mathbf{4}_{s\text{-}Br}$	26.20	33.20	–	22.87	27.99	25.51	25.87	1	1.49	6.05
$\mathbf{4}_{t\text{-}Br}$	16.30	58.50	–	20.64	21.89	20.62	20.67	0	2.00	6.59

[a] ZPE not included.
[b] The lowest energy minimum is set at 0.00 kcal/mol; the original total energies (hartrees) corresponding to the lowest energy minimum $\mathbf{1}_{s\text{-}Br}$ at various levels of theory: (1) −3439.699964, (2) −3440.081425, (3) –, (4)−3443.255181, (5) −3440.138998, (6) −3440.140596, (7) −3440.139977.

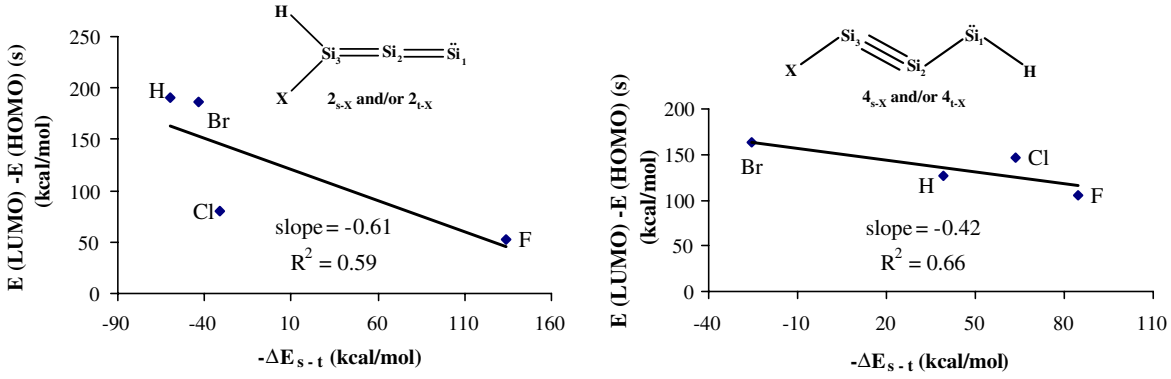

Fig. 6. Correlations between the LUMO–HOMO energy gaps (kcal/mol) of the singlet $XHSi_3$ silylenes and their corresponding singlet–triplet energy separations, $\Delta E_{s\text{-}t,X}$ (kcal/mol) for $\mathbf{2_{s\text{-}X}}$, $\mathbf{2_{t\text{-}X}}$ (left) and $\mathbf{4_{s\text{-}X}}$, $\mathbf{4_{t\text{-}X}}$ (right), for X = H, F, Cl and Br, calculated at MP2/6-311+G** (R^2 = correlation coefficient).

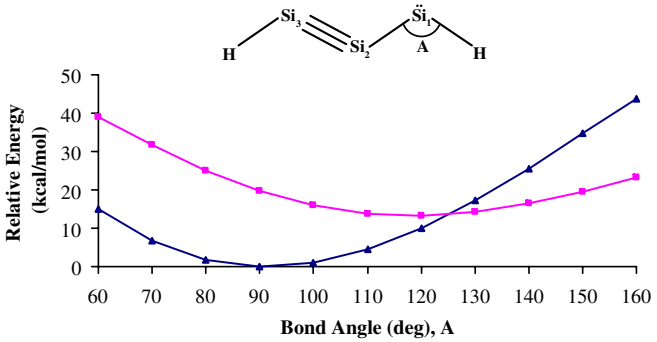

Fig. 7. MP2/6-311+G** relative energies (kcal/mol) of the singlet (**s**,▲) and triplet (**t**,■) states of $\mathbf{3_{s\text{-}H}}$ and $\mathbf{3_{t\text{-}H}}$, silylenes plotted as a function of the divalent bond angle ∠H–Si_1–Si_2 (°).

X are negligible and variations of Si–Si and/or Si=Si bond lengths of singlet $\mathbf{1_{s-X}}$ as a function of X are small (Figs. 2–5). This is due to the aromatic character of the singlet species $\mathbf{1_{s-X}}$ along with the less significance of canonical forms containing charge separations (Schemes 1 and 2). In contrast, in triplet $\mathbf{1_{t\text{-}H}}$ the Si_1–Si_2 and Si_1–Si_3 bond lengths are different (2.39 and 2.19 Å, respectively), indicating that only the Si_1–Si_2 bond interacts with the divalent center, consequently the corresponding Si_2=Si_3 double bond becomes longer to the extent of 2.32 Å. This is, considering the common Si–Si bond distance is 2.33 Å, while Si=Si bond distances vary from 2.14 to 2.25 Å. Similarly, in triplet $\mathbf{1_{t\text{-}F}}$ and/or $\mathbf{1_{t\text{-}Cl}}$ only the Si_1–Si_2 bond, which is attached to the halogen, interacts with the divalent center. This interaction in triplet $\mathbf{1_{t\text{-}Br}}$ is so large that causes the cleavage of Si_2=Si_3 double bond (Fig. 5). Every Si_2=Si_3 bond length in the triplet species $\mathbf{1_{t\text{-}X}}$ is longer than its corresponding Si_2=Si_3 bond length in the corresponding singlet $\mathbf{1_{s\text{-}X}}$. The MP2/6-311+G** calculated atomic charges confirm this findings, since Si_3 in $\mathbf{1_{t\text{-}H}}$ is more negative than Si_2 (Tables 5 and 6). Moreover, the divalent atom Si_1 in singlet $\mathbf{1_{s\text{-}H}}$ is more positive than Si_2 and/or Si_3, while in triplet $\mathbf{1_{t\text{-}H}}$ divalent Si_1 is more negative than Si_2 and/or Si_3. The

Table 5
MP2/6-311+G** calculated NBO atomic charges for singlet states of $XHSi_3$ species (X = H, F, Cl and Br)

Atom	Structure														
	$\mathbf{1_{s\text{-}H}}$	$\mathbf{1_{s\text{-}F}}$	$\mathbf{1_{s\text{-}Cl}}$	$\mathbf{1_{s\text{-}Br}}$	$\mathbf{2_{s\text{-}H}}$	$\mathbf{2_{s\text{-}F}}$	$\mathbf{2_{s\text{-}Cl}}$	$\mathbf{2_{s\text{-}Br}}$	$\mathbf{3_{s\text{-}H}}$	$\mathbf{3_{s\text{-}F}}$	$\mathbf{3_{s\text{-}Cl}}$	$\mathbf{3_{s\text{-}Br}}$	$\mathbf{4_{s\text{-}F}}$	$\mathbf{4_{s\text{-}Cl}}$	$\mathbf{4_{s\text{-}Br}}$
Si_1	0.11	0.06	0.13	0.14	0.20	0.19	−0.06	0.27	0.15	1.25	0.38	0.60	0.16	0.24	0.30
Si_2	0.09	0.76	0.27	0.14	−0.18	−0.25	0.39	−0.21	−0.04	−0.60	−0.10	−0.32	−0.24	−0.23	−0.33
Si_3	0.09	0.01	0.09	0.11	0.27	0.85	0.15	0.39	0.14	0.08	0.13	0.32	0.87	0.38	0.61
X	−0.14	−0.69	−0.35	−0.26	−0.14	−0.67	−0.37	−0.28	−0.12	−0.66	−0.32	−0.41	−0.68	−0.31	−0.41
H	−0.14	−0.14	−0.14	−0.14	−0.15	−0.12	−0.10	−0.17	−0.13	−0.08	−0.08	−0.18	−0.10	−0.08	−0.17

Table 6
MP2/6-311+G** calculated NBO atomic charges for triplet states of $XHSi_3$ species (X = H, F, Cl and Br)

Atom	Structure														
	$\mathbf{1_{t\text{-}H}}$	$\mathbf{1_{t\text{-}F}}$	$\mathbf{1_{t\text{-}Cl}}$	$\mathbf{1_{t\text{-}Br}}$	$\mathbf{2_{t\text{-}H}}$	$\mathbf{2_{t\text{-}F}}$	$\mathbf{2_{t\text{-}Cl}}$	$\mathbf{2_{t\text{-}Br}}$	$\mathbf{3_{t\text{-}H}}$	$\mathbf{3_{t\text{-}F}}$	$\mathbf{3_{t\text{-}Cl}}$	$\mathbf{3_{t\text{-}Br}}$	$\mathbf{4_{t\text{-}F}}$	$\mathbf{4_{t\text{-}Cl}}$	$\mathbf{4_{t\text{-}Br}}$
Si_1	−0.30	−0.06	−0.70	−0.09	0.20	0.09	0.20	−0.60	−0.72	−0.31	−0.52	−0.61	−0.76	−0.69	0.33
Si_2	−0.13	−0.21	0.44	0.44	−0.22	−0.20	−0.20	0.13	0.64	0.48	0.56	0.64	0.50	0.56	0.10
Si_3	−0.23	−0.24	−0.55	−0.09	0.32	1.06	0.61	−0.30	−0.72	−0.67	−0.68	−0.72	−0.28	−0.51	0.09
X	−0.23	−0.42	−0.16	−0.38	−0.15	−0.71	−0.41	−0.16	−0.10	−0.39	−0.26	−0.22	−0.39	−0.26	−0.38
H	−0.11	−0.07	−0.03	−0.22	−0.16	−0.25	−0.20	−0.06	−0.10	−0.11	−0.11	−0.10	−0.07	−0.11	−0.14

Table 7
The NBO hybridization for singlet (**s**) and triplet (**t**) states of cyclic $\mathbf{1_{s\text{-}X}}$ and $\mathbf{1_{t\text{-}X}}$ structures (X = H, F, Cl and Br) calculated at MP2/6-311+G**

Bond	$\mathbf{1_{s\text{-}H}}$	$\mathbf{1_{t\text{-}H}}$	$\mathbf{1_{s\text{-}F}}$	$\mathbf{1_{t\text{-}F}}$	$\mathbf{1_{s\text{-}Cl}}$	$\mathbf{1_{t\text{-}Cl}}$	$\mathbf{1_{s\text{-}Br}}$	$\mathbf{1_{t\text{-}Br}}$
$\sigma_{Si_1-Si_2}$	$s^1p^{11.00}d^{0.09}$	$s^1p^{7.00}d^{0.05}$	$s^1p^{12.43}d^{0.10}$	$s^1p^{8.21}d^{0.06}$	$s^1p^{11.95}d^{0.10}$	$s^1p^{7.92}d^{0.06}$	$s^1p^{11.79}d^{0.10}$	$s^1p^{5.49}d^{0.04}$
$\sigma_{Si_1-Si_3}$	$s^1p^{11.00}d^{0.09}$	$s^1p^{7.00}d^{0.05}$	$s^1p^{9.98}d^{0.10}$	$s^1p^{10.66}d^{0.09}$	$s^1p^{10.55}d^{0.09}$	$s^1p^{11.47}d^{0.08}$	$s^1p^{10.64}d^{0.09}$	$s^1p^{5.87}d^{0.05}$

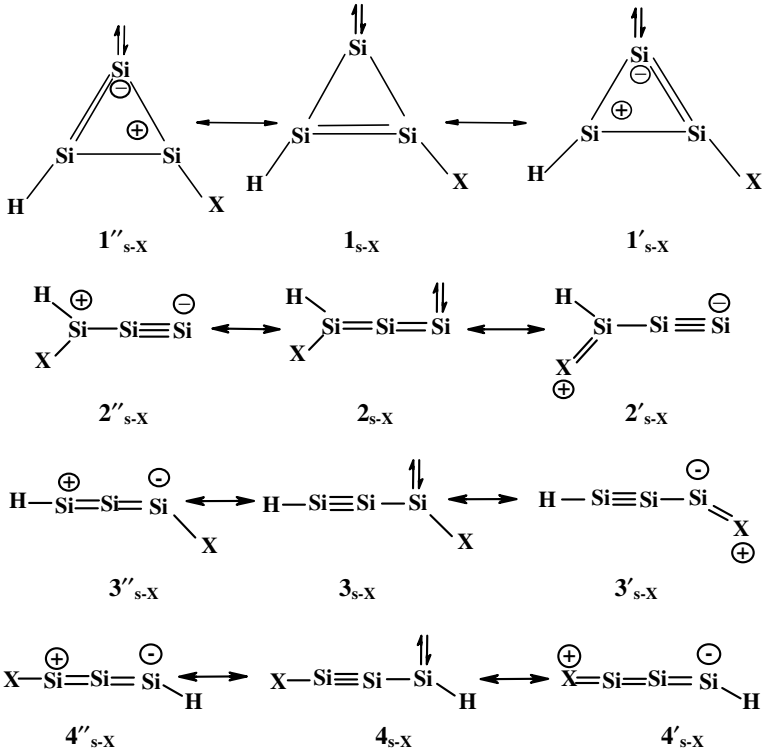

Scheme 1. The most significant canonical forms for singlet state silylenes: $\mathbf{1_{s\text{-}X}}$, $\mathbf{2_{s\text{-}X}}$, $\mathbf{3_{s\text{-}X}}$ and $\mathbf{4_{s\text{-}X}}$.

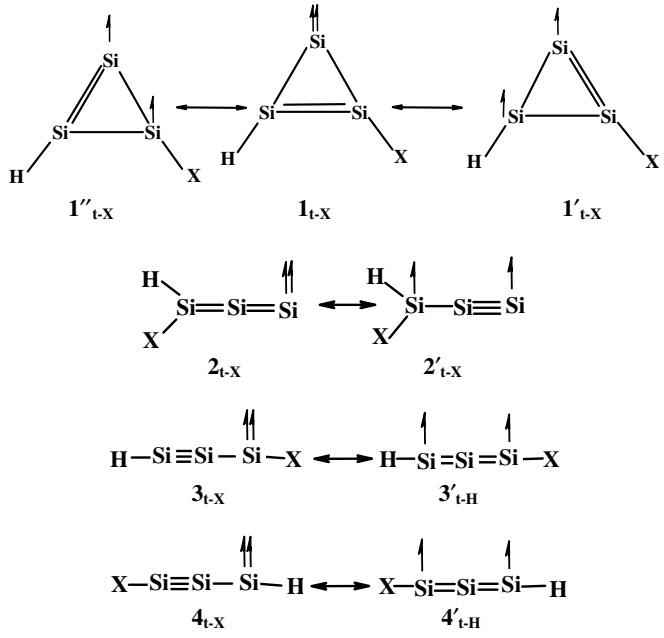

Scheme 2. The most significant canonical forms for triplet state silylenes: $\mathbf{1_{t\text{-}X}}$, $\mathbf{2_{t\text{-}X}}$, $\mathbf{3_{t\text{-}X}}$ and $\mathbf{4_{t\text{-}X}}$.

$\angle Si_2Si_1Si_3$ divalent angle in all triplet $\mathbf{1_{t\text{-}X}}$ species is larger than its corresponding singlet $\mathbf{1_{s\text{-}X}}$. This is in consistent with the other reports, on many related acyclic carbenic and silylenic systems, while it is in contrast to the results of the corresponding cyclic carbenic and/or silylenic systems [8,29–35]. This discrepancy may be rationalized by considering the electronic structures and hybridizations of the corresponding bonds, attached to the divalent center. For instance, the strictly localized natural bond orbitals (NBO) of the σ molecular orbitals show more p character for $\mathbf{1_{s\text{-}X}}$ divalent bonds than those of $\mathbf{1_{t\text{-}X}}$ (Table 7).

The CCSD(T)/6-311++G** calculated order of singlet–triplet energy gaps ($\Delta E_{s-t,X}$), between $\mathbf{1_{s\text{-}X}}$ and $\mathbf{1_{t\text{-}X}}$ is: $\Delta E_{s-t,F}$ (63.72 kcal/mol) > $\Delta E_{s-t,H}$ (53.13 kcal/mol) > $\Delta E_{s-t,Cl}$ (46.74 kcal/mol) > $\Delta E_{s-t,Br}$ (30.48 kcal/mol) (Tables 1–4). Evidently, the most electronegative substituent has the highest $\Delta E_{s-t,X}$.

Among acyclic silylenes, the first structures considered are the singlet states and the triplet states of 3-X-1,2,3-trisilapropadienylidene ($\mathbf{2_{s\text{-}X}}$ vs. $\mathbf{2_{t\text{-}X}}$, Fig. 1). Except for the more electronegative atom (fluorine, $\mathbf{2_{s\text{-}F}}$), singlet states $\mathbf{2_{s\text{-}X}}$ appear more stable than their corresponding triplets $\mathbf{2_{t\text{-}X}}$ (Tables 1–4). The six ab initio methods employed show

triplet silylene $\mathbf{2_{t\text{-}F}}$ as the real isomer which is more stable than its corresponding singlet $\mathbf{2_{s\text{-}F}}$. Moreover, the singlet state $\mathbf{2_{s\text{-}F}}$ has one imaginary frequency and is not a real isomer. In other words, all the odds are in favor of existence of the triplet silylene $\mathbf{2_{t\text{-}F}}$, while they are against the singlet $\mathbf{2_{s\text{-}F}}$. Singlet state $\mathbf{2_{s\text{-}H}}$ undergoes a rearrangement upon optimization, at MP2/6-311+G** level, forming a rather long linkage from Si_1 to Si_3 (2.46 Å) and transforms into a cyclic structure (Fig. 2). Such rearrangement occurs for all $\mathbf{2_{s\text{-}X}}$ structures upon optimization at B3LYP/6-311++G** level (supplementary information). Interestingly, in all the allenic moieties of both $\mathbf{2_{s\text{-}X}}$ and/or $\mathbf{2_{t\text{-}X}}$, the $\angle Si_1Si_2Si_3$ silaallenic angle is bent [25] and the extent of this bending is a function of X which is inversely proportional to electro-negativity: Br > Cl > F. The Si_1–Si_2 bond lengths in $\mathbf{2_{s\text{-}X}}$ species become longer as the electro-negativity of halogen reduces (Br > Cl > F). Among the $\mathbf{2_{t\text{-}X}}$ species, $\mathbf{2_{t\text{-}F}}$ (a minimum) and $\mathbf{2_{t\text{-}Cl}}$ (a transition state) have C_1 symmetry while, $\mathbf{2_{t\text{-}H}}$ and $\mathbf{2_{t\text{-}Br}}$ are planar with C_s symmetry (Figs. 2–5). The triplet structure of $\mathbf{2_{t\text{-}Br}}$ is very bent (73.6°) and possibly tends to become a cyclic structure like $\mathbf{2_{s\text{-}H}}$. Triplet silylene $\mathbf{2_{t\text{-}F}}$ is non-planar, with a bent silaallenic angle (137.4°), and long Si_2=Si_3 bond length (2.31 Å), which is longer than the normal Si=Si double bonds. The lower charge on Si_1 along with the higher charge on Si_3 atoms of $\mathbf{2_{t\text{-}F}}$, compared to $\mathbf{2_{s\text{-}F}}$, suggest the higher importance of resonance canonical forms $\mathbf{2''_{t\text{-}F}}$ and $\mathbf{2''_{s\text{-}F}}$ (Schemes 1 and 2; Tables 5 and 6).

The CCSD(T)/6-311++G** calculated order of singlet–triplet energy gaps, $\Delta E_{s\text{-}t,X}$, between $\mathbf{2_{s\text{-}X}}$ and $\mathbf{2_{t\text{-}X}}$ is: $\Delta E_{s\text{-}t,F}$ (−133.54 kcal/mol) > $\Delta E_{s\text{-}t,H}$ (33.10 kcal/mol) > $\Delta E_{s\text{-}t,Br}$ (32.24 kcal/mol) > $\Delta E_{s\text{-}t,Cl}$ (31.33 kcal/mol) (Tables 1–4). Apparently, fluorine has an extraordinary $\Delta E_{s\text{-}t,X}$ between the triplet minimum $\mathbf{2_{t\text{-}F}}$ and the transition state $\mathbf{2_{s\text{-}F}}$.

The second acyclic silylenes considered are the singlet and triplet states of 1-X-1,2,3-trisilapropargylene ($\mathbf{3_{s\text{-}X}}$ and $\mathbf{3_{t\text{-}X}}$), where halogens are directly bonded to the silylenic divalent center (Fig. 1). All singlet $\mathbf{3_{s\text{-}X}}$ as well as the triplet states of $\mathbf{3_{t\text{-}H}}$ and $\mathbf{3_{t\text{-}Br}}$ show negative force constants and are not real isomers and exist as transition states (Tables 1–4). However, CCSD(T) calculations reveal that singlet $\mathbf{3_{s\text{-}X}}$ (X = F and Br) are more stable than their corresponding triplet $\mathbf{3_{t\text{-}X}}$. Conversely, triplet states $\mathbf{3_{t\text{-}X}}$ (for X = H and Cl) are more stable than their corresponding singlet $\mathbf{3_{s\text{-}X}}$. Such stability of triplet silylenes, compared to their corresponding singlet states, is remarkable and can be justified based on the electropositivity of the substituted divalent Si atom, along with the presence of a triple bond (Si≡Si) attached to the silylenic center. Energy gaps between $\mathbf{3_{s\text{-}X}}$ and $\mathbf{3_{t\text{-}X}}$, calculated at CCSD(T)/6-311++G** level, appear as: $\Delta E_{s-t,Cl}$ (−59.22 kcal/mol) > $\Delta E_{s-t,H}$ (−44.20 kcal/mol) > $\Delta E_{s-t,F}$ (35.19 kcal/mol) > $\Delta E_{s-t,Br}$ (26.77 kcal/mol) (Tables 1–4). This trend demonstrates the stabilizing of singlet silylenes, due to the effects of electro-negativity, suggested by Gaspar [48]. Contrary to alkynes, the substituents attached to the Si≡Si moiety are not arranged in a linear fashion. They are "*trans*-bent" with $\angle Si_1Si_2Si_3$ bond angles varying between 99.4° and 175.3°. This result is comparable with the Sekiguchi findings for the first synthesized disilyne compound [26]. Halogens in the α position of both $\mathbf{3_{s\text{-}X}}$ and $\mathbf{3_{t\text{-}X}}$ appear to have a pronounced effect on the corresponding Si_1–Si_2 and Si_2–Si_3 bond lengths (Figs. 2–5). The Si_1–Si_2 bond length in $\mathbf{3_{s\text{-}X}}$ varies as: $\mathbf{3_{s\text{-}F}}$ (2.38 Å) > $\mathbf{3_{s\text{-}Br}}$ (2.34 Å) > $\mathbf{3_{s\text{-}H}}$ (2.12 Å) $\mathbf{3_{s\text{-}Cl}}$ (2.09 Å). The Si_2–Si_3 bond length in $\mathbf{3_{s\text{-}X}}$ varies as: $\mathbf{3_{s\text{-}Cl}}$ (2.16 Å) > $\mathbf{3_{s\text{-}H}}$ (2.13 Å) > $\mathbf{3_{s\text{-}F}}$ (2.11 Å) > $\mathbf{3_{s\text{-}Br}}$ (2.09 Å) (Figs. 2–5). One may justify these trends by considering the canonical forms in which the triple bond Si≡Si delivers its π electrons into the vacant p orbital of the divalent Si. However, in the cases of $\mathbf{3_{s\text{-}F}}$ and $\mathbf{3_{s\text{-}Br}}$, where the halogens can directly stabilize the silylenic center, this interaction is less pronounced (Scheme 1). Delocalization of Si≡Si π electrons, through the divalent center, causes the observed disordered trend of the divalent angles $\angle Si_2Si_1X$ [8,24]. Upon optimization, no rearrangement or ruptures are observed in silylenic species with structures $\mathbf{3_{s\text{-}X}}$ and/or $\mathbf{3_{t-X}}$ (Fig. 5). Triplet states $\mathbf{3_{t\text{-}F}}$ and $\mathbf{3_{t\text{-}Cl}}$ have a *trans* arrangement of substituents around the Si_1–Si_2≡Si_3 moiety with no symmetry (C_1). The remaining $\mathbf{3_{t\text{-}H}}$, $\mathbf{3_{t\text{-}Br}}$ as well as $\mathbf{3_{s\text{-}X}}$ species have at least a plane of symmetry (C_s). In contrast to $\mathbf{3_{s\text{-}F}}$, which is a transition state, the corresponding triplet silylene $\mathbf{3_{t\text{-}F}}$ which can be accessible for being a minimum on its energy surfaces, has a structure closer to $\mathbf{3_{t\text{-}Cl}}$, but with more bending in its Si_1–Si_2≡Si_3 moiety ($\angle Si_1Si_2Si_3 = 112.5°$).

The last acyclic structures considered are the singlet and triplet states of 3-X-1,2,3-trisilapropargylene, ($\mathbf{4_{s\text{-}X}}$ and $\mathbf{4_{t\text{-}X}}$) (Fig. 1). This structure is closely related to $\mathbf{3_{s\text{-}X}}$ and $\mathbf{3_{t\text{-}X}}$, respectively. Besides, when X = H, they become exactly the same. Fascinatingly, all the employed calculation methods indicate that for X = Cl, the triplet state $\mathbf{4_{t\text{-}Cl}}$, is more stable than its corresponding singlet $\mathbf{4_{s\text{-}Cl}}$, which shows a negative force constant and is a transition state (Table 3). Likewise, when X = Br, all calculation methods (except MP2) show triplet state $\mathbf{4_{t\text{-}Br}}$, which is a minimum on its energy surface, more stable than its corresponding singlet state $\mathbf{4_{s\text{-}Br}}$, which is a transition state (Table 4). However, when X = F, both $\mathbf{4_{t\text{-}F}}$ and $\mathbf{4_{t\text{-}F}}$ are transition states. For these transition states all calculation methods except B3LYP, show the triplet state $\mathbf{4_{t\text{-}F}}$ to be more stable than its corresponding singlet $\mathbf{4_{s\text{-}F}}$ (Table 2). Reaching for stable triplet silylenes in this case is very interesting. At B3LYP level, all $\mathbf{4_{t\text{-}X}}$ silylenes appear to rearrange to cyclic forms (supplementary information), while at MP2/6-311+G** level, only $\mathbf{4_{t\text{-}Br}}$ rearranges to a cyclic form (Figs. 2–5). The MP2/6-311+G** calculations show the triplet silylene $\mathbf{4_{t\text{-}Cl}}$, to be non-planar with its Si_1≡Si_2–Si_3 moiety considerably bent ($\angle Si_1Si_2Si_3 = 107.9°$), with its Si_3–Si_2 bond length being 2.21 Å, and its Si_1–Si_2 bond length being somewhat shorter (2.14 Å) (Fig. 4). This indicates that the electron delocalization anticipated between triple bond Si≡Si and divalent center is less significant in $\mathbf{4_{t\text{-}Cl}}$, compared to the corresponding $\mathbf{4_{s\text{-}Cl}}$ and/or $\mathbf{3_{t\text{-}Cl}}$ (Schemes 1, 2). The CCSD(T)/6-311+G** calculated order of singlet–triplet energy gaps, appearing between $\mathbf{4_{s\text{-}X}}$ and $\mathbf{4_{t\text{-}X}}$ is: $\Delta E_{s\text{-}t,Cl}$

(−58.14 kcal/mol) > $\Delta E_{s\text{-}t,F}$ (−21.56 kcal/mol) > $\Delta E_{s\text{-}t,Br}$ (−5.20 kcal/mol) (Tables 1–4).

3.2. Comparisons within isomeric sets of $XHSi_3$ silylenes for X = H, F, Cl and Br

We begin for species with X = H. The CCSD(T)/6-311++G** calculated relative stability for H_2Si_3 species is: $\mathbf{1}_{s-H}$ (0.0 kcal/mol) > $\mathbf{2}_{s\text{-}H}$ (5.07 kcal/mol) > $\mathbf{2}_{t\text{-}H}$ (38.71 kcal/mol) > $\mathbf{3}_{t\text{-}H}$ (40.01 kcal/mol) $\mathbf{1}_{t\text{-}H}$ (53.13 kcal/mol) > $\mathbf{3}_{s\text{-}H}$ (90.21 kcal/mol) (Table 1). In contrast to C_2HSiX silylenic analogues, where all singlet states appear more stable than their corresponding triplet states [32], here triplet state $\mathbf{3}_{t\text{-}H}$ turns out to be more stable than its corresponding singlet states $\mathbf{3}_{s\text{-}H}$. The structure of lowest energy, and presumably the global minimum of the hyper-surface of H_2Si_3 emerges as singlet X-1,2,3-trisila-1-cyclopropenylidene, $\mathbf{1}_{s\text{-}H}$; which is consistent with the results reported by Gordon and Schriver [49]. In fact, $\mathbf{1}_{s\text{-}H}$ has a σ^2 silylenic center which enables it to show an aromatic character. Hence, $\mathbf{2}_{s\text{-}H}$ is less stable than $\mathbf{1}_{s\text{-}H}$, due to its lack of such aromatic character. The stabilizing effect of an additional Si–Si bond in $\mathbf{2}_{s\text{-}H}$, as a replacement for Si–H bond in the transition state $\mathbf{3}_{s\text{-}H}$ makes the former more stable than the latter.

The MP2/6-311+G** calculated relative stability for $FHSi_3$ species is: $\mathbf{1}_{s\text{-}F}$ (0.00 kcal/mol) > $\mathbf{3}_{s\text{-}F}$ (24.77 kcal/mol) > $\mathbf{4}_{t\text{-}F}$ (31.91 kcal/mol) > $\mathbf{2}_{t\text{-}F}$ (44.96 kcal/mol) > $\mathbf{1}_{t\text{-}F}$ (52.23 kcal/mol) > $\mathbf{3}_{t\text{-}F}$ (59.96 kcal/mol) > $\mathbf{4}_{s\text{-}F}$ (116.75 kcal/mol) > $\mathbf{2}_{s\text{-}F}$ (178.50 kcal/mol) (Table 2). Interestingly, the stability order of $FHSi_3$ silylenes appears quite different from the above stability trend of H_2Si_3, and is in clear contrast to analogues C_3FH carbenes [29]. Moreover, with the most electronegative halogen, singlet species of $\mathbf{1}_{s\text{-}F}$ and $\mathbf{3}_{s\text{-}F}$ are more stable than their corresponding triplet states ($\mathbf{1}_{t\text{-}F}$ and $\mathbf{3}_{t\text{-}F}$, respectively). The global minimum for the set of $FHSi_3$ silylenes appears to be singlet cyclic 2-X-1,2,3-trisilacyclopropenylidene, $\mathbf{1}_{s\text{-}F}$, which is highly stabilized by fluorine attached to the three-membered aromatic ring. Nevertheless, resonance stabilization along with the electro-negativity may justify the higher stability of the transition state $\mathbf{3}_{s\text{-}F}$ over $\mathbf{4}_{t\text{-}F}$.

The MP2/6-311+G** calculated relative stability of $ClHSi_3$ species is: $\mathbf{1}_{s\text{-}Cl}$ (0.00 kcal/mol) > $\mathbf{2}_{s\text{-}Cl}$ (28.96 kcal/mol) > $\mathbf{1}_{t\text{-}Cl}$ (53.07 kcal/mol) > $\mathbf{3}_{t\text{-}Cl}$ (58.80 kcal/mol) > $\mathbf{2}_{t\text{-}Cl}$ (60.29 kcal/mol) > $\mathbf{4}_{t\text{-}Cl}$ (61.01 kcal/mol) > $\mathbf{4}_{s\text{-}Cl}$ (124.73 kcal/mol) > $\mathbf{3}_{s\text{-}Cl}$ (139.85 kcal/mol) (Table 3). Again, the global minimum for the set of $ClHSi_3$ silylenes appears to be the singlet cyclic 2-X-1,2,3-trisilacyclopropenylidene, $\mathbf{1}_{s\text{-}Cl}$. The shorter range of energy differences between the isomers involved may be due to lower stabilizing effect of chlorine, than fluorine, on the singlet states. The triplet silylene $\mathbf{3}_{t\text{-}Cl}$ (which is a real isomer), is 81.05 kcal/mol (at MP2 level) more stable, than its corresponding singlet $\mathbf{3}_{s\text{-}Cl}$. Also, triplet $\mathbf{4}_{t\text{-}Cl}$ appears more stable than the corresponding singlet states $\mathbf{4}_{s\text{-}Cl}$.

CCSD(T)/6-311++G** calculated relative stability of $BrHSi_3$ silylenes, is: $\mathbf{1}_{s\text{-}Br}$ (0.00 kcal/mol) > $\mathbf{2}_{s\text{-}Br}$ (6.54 kcal/mol) > $\mathbf{4}_{t\text{-}Br}$ (20.67/mol) > $\mathbf{3}_{s\text{-}Br}$ (24.09 kcal/mol) > $\mathbf{4}_{s\text{-}Br}$ (25.78 kcal/mol) > $\mathbf{1}_{t\text{-}Br}$ (30.48 kcal/mol) > $\mathbf{2}_{t\text{-}Br}$ (43.78 kcal/mol) > $\mathbf{3}_{t\text{-}Br}$ (50.86 kcal/mol) (Table 4). Again except for the global minimum location, this is a different trend than those found for both $ClHSi_3$ and $FHSi_3$. The global minimum for the set of $BrHSi_3$ appears to be singlet cyclic X-1,2,3-trisilacyclopropenylidene, $\mathbf{1}_{s-Br}$. Triplet state $\mathbf{4}_{t\text{-}Br}$ appears more stable than its corresponding singlet states $\mathbf{4}_{s\text{-}Br}$.

The MP2/6-311+G** calculated dipole moments for singlet (**s**) and triplet (**t**) states of $XHSi_3$ silylenes are presented in Tables 1–4. For silylenes with X = H and F, all singlet states have higher dipole moments than their corresponding triplet states. In contrast, the triplet states $\mathbf{3}_{t\text{-}Cl}$, $\mathbf{1}_{t\text{-}Br}$, $\mathbf{3}_{t\text{-}Br}$ and $\mathbf{4}_{t\text{-}Br}$ appear more polar than their corresponding singlet states. In H_2Si_3 series, the most polar silylene is the singlet $\mathbf{1}_{s\text{-}H}$ (1.69 D). This again confirms the aromaticity encountered in the singlet $\mathbf{1}_{s\text{-}H}$. The highest polar silylene among all appears to be the planar singlet $\mathbf{2}_{s\text{-}F}$ (3.45 D) Moreover, $\mathbf{1}_{t\text{-}H}$ and $\mathbf{3}_{t\text{-}H}$ are almost non-polar.

4. Conclusion

Singlet–triplet energy separations ($\Delta E_{t\text{-}s,X}$) in silylenic $XHSi_3$ species, are compared and contrasted, at seven ab initio and DFT levels of theory: B3LYP/6-311++G**, HF/6-311++G**, MP3/6-311G*, MP2/6-311+G**, MP4(SDTQ)/6-311++G**, QCISD(T)/6-311++G** and CCSD(T)/6-311++G** (where X = H, F, Cl and Br). 2-X-1,2,3-trisilacyclopropenylidene (**1**) is considered as the cyclic skeleton for four singlet $\mathbf{1}_{s-X}$ as well as four triplet $\mathbf{1}_{t\text{-}X}$ states of $XHSi_3$. Likewise, three acyclic structures consisting of 3-X-1,2,3-trisilapropadienylidene (**2**); 1-X-1,2,3-trisilapropargylene (**3**); and 3-X-1,2,3-trisilapropargylene (**4**), are considered for 11 singlet ($\mathbf{2}_{s\text{-}X}$, $\mathbf{3}_{s\text{-}X}$ and $\mathbf{4}_{s\text{-}X}$, respectively) and 11 triplet ($\mathbf{2}_{t\text{-}X}$, $\mathbf{3}_{t\text{-}X}$ and $\mathbf{4}_{t\text{-}X}$, respectively) states of silylenic $XHSi_3$. The 17 species $\mathbf{1}_{t\text{-}H}$, $\mathbf{1}_{t\text{-}F}$, $\mathbf{1}_{t\text{-}Cl}$, $\mathbf{1}_{t\text{-}Br}$, $\mathbf{2}_{s\text{-}F}$, $\mathbf{2}_{t\text{-}H}$, $\mathbf{2}_{t\text{-}Br}$, $\mathbf{3}_{s\text{-}H}$, $\mathbf{3}_{s\text{-}F}$, $\mathbf{3}_{s\text{-}Cl}$, $\mathbf{3}_{s\text{-}Br}$, $\mathbf{3}_{t\text{-}H}$, $\mathbf{3}_{t\text{-}Br}$, $\mathbf{4}_{s\text{-}F}$, $\mathbf{4}_{t\text{-}F}$, $\mathbf{4}_{s\text{-}Cl}$ and $\mathbf{4}_{s\text{-}Br}$ exist as transition states. Linear correlations are found between the LUMO–HOMO energy gaps of the singlet silylenes $\mathbf{2}_{s\text{-}X}$ and/or $\mathbf{4}_{s\text{-}X}$, and their corresponding singlet–triplet energy separations, calculated at MP2/6-311+G**. The CCSD(T) calculated order of $\Delta E_{t\text{-}s,X}$ for cyclic species, $\mathbf{1}_{t\text{-}X} - \mathbf{1}_{s\text{-}X}$, as a function of X is F > H > Cl > Br. In contrast, the order of singlet–triplet energy gaps, for acyclic structures **2** is: F > H > Br > Cl; while for **3** is: Cl > H > F > Br; and for **4** is Cl > F > Br. The order of stability for six structures of H_2Si_3 is $\mathbf{1}_{s\text{-}H} > \mathbf{2}_{s\text{-}H} > \mathbf{2}_{t\text{-}H} > \mathbf{3}_{t\text{-}H} > \mathbf{1}_{t\text{-}H} > \mathbf{3}_{s\text{-}H}$. The stability order for eight structures of $FHSi_3$ is: $\mathbf{1}_{s\text{-}F} > \mathbf{3}_{s\text{-}F} > \mathbf{4}_{t\text{-}F} > \mathbf{2}_{t\text{-}F} > \mathbf{1}_{t\text{-}F} > \mathbf{3}_{t\text{-}F} > \mathbf{4}_{s\text{-}F} > \mathbf{2}_{s\text{-}F}$. The stability order for $ClHSi_3$ structures is: $\mathbf{1}_{s\text{-}Cl} > \mathbf{2}_{s\text{-}Cl} > \mathbf{1}_{t\text{-}Cl} > \mathbf{3}_{t\text{-}Cl} > \mathbf{2}_{t\text{-}Cl} > \mathbf{4}_{t\text{-}Cl} > \mathbf{4}_{s\text{-}Cl} > \mathbf{3}_{s\text{-}Cl}$. Finally the stability order for $BrHSi_3$ structures is: $\mathbf{1}_{s\text{-}Br} > \mathbf{2}_{s\text{-}Br} > \mathbf{4}_{t\text{-}Br} > \mathbf{3}_{s\text{-}Br} > \mathbf{4}_{s\text{-}Br} > \mathbf{1}_{t\text{-}Br} > \mathbf{2}_{t\text{-}Br} > \mathbf{3}_{t\text{-}Br}$. Structures of the lowest energy appear to be $\mathbf{1}_{s\text{-}X}$. All ab initio calculations show triplet silylenes $\mathbf{4}_{t\text{-}Cl}$, $\mathbf{3}_{t\text{-}Cl}$ as well as $\mathbf{2}_{t\text{-}F}$ more stable than their corresponding singlet states. Also, triplet state of $\mathbf{3}_{t\text{-}F}$ is possibly accessible for being an energy minimum while its corresponding singlet is transition state. The stability trends demonstrate the triplet state stabilization

via two electropositive tetravalent Si atoms, as well as singlet state stabilization through the resonance effects and/or inductive effects of halogens. Some discrepancies are observed between energetic and/or structural results of DFT vs. ab initio methods.

Acknowledgments

We acknowledge the useful discussion and hints of A. Ghaderi (Imam Hossein University). Special thanks are due to Kh. Didehban and Dr. Y. Fatholahi (Tarbiat Modares University), for their cordial assistance in providing the necessary means to finish this manuscript.

Appendix A. Supplementary data

Supplementary data associated with this article can be found, in the online version, at doi:10.1016/j.jorganchem.2005.12.045.

References

[1] M. Ishikawa, M. Kumada, Adv. Organomet. Chem. 19 (1981) 51.
[2] P. Riviere, A. Castel, J. Satgt, J. Am. Chem. Soc. 102 (1980) 5413.
[3] M.Z. Kassaee, S. Arshadi, E. Vessally, J. Organomet. Chem. 690 (2005) 3427.
[4] G. Olbrich, Chem. Phys. Lett. 73 (1980) 110.
[5] P. Saxe, H.F. Schaefer III, N. Handy, J. Phys. Chem. 85 (1981) 745.
[6] M.S. Gordon, M.W. Schmidt, Chem. Phys. Lett. 132 (1986) 294.
[7] J. Kalcher, A.F. Sax, J. Mol. Struct. (Theochem) 253 (1992) 287.
[8] H.P. Reisenauer, G. Maier, A. Reimann, R.W. Hoffmann, Angew. Chem., Int. Ed. 96 (1984) 596.
[9] J.R. Redondo, P. Redondo, A. Largo, J. Mol. Struct. (Theochem) 621 (2003) 59.
[10] M.W. Schmidt, P.N. Truong, M.S. Gordon, J. Am. Chem. Soc. 109 (1987) 5217.
[11] P.V.R. Schleyer, D. Kost, J. Am. Chem. Soc. 110 (1988) 2105.
[12] T.C. Klebach, R. Lourens, F. Bickelhaupt, J. Am. Chem. Soc. 100 (1978) 4886.
[13] A.G. Brook, F. Abdesaken, B. Gutekunst, G. Gutekunst, R.K. Kallury, J. Chem. Soc., Chem. Commun. (1981) 191.
[14] R. West, M.J. Fink, J. Michl, Science 214 (1981) 1343.
[15] M. Yoshifuji, I. Shima, N. Inamoto, K. Hirotsu, T. Higuchi, J. Am. Chem. Soc. 103 (1981) 4587.
[16] L.C. Snyder, Z.R. Wasserman, J. Am. Chem. Soc. 101 (1979) 5222.
[17] J.C. Barthelat, G. Trinquier, G. Bertrand, J. Am. Chem. Soc. 101 (1979) 3785.
[18] A.C. Hopkinson, M.H. Lien, J. Chem. Soc., Chem. Commun. (1980) 107.
[19] M.S. Gordon, J. Am. Chem. Soc. 102 (1980) 7419.
[20] T. Iwamoto, M. Tamura, C. Kabuto, M. Kira, Organomettallics 22 (2003) 2342.
[21] T. Iwamoto, M. Tamura, C. Kabuto, M. Kira, Science 290 (2000) 504.
[22] K. Sakamoto, J. Ogasawara, Y. Kon, T. Sunagawa, M. Kira, Angew. Chem., Int. Ed. 41 (2002) 1402.
[23] Y. Kon, J. Ogasawara, K. Sakamoto, C. Kabuto, M. Kira, J. Am. Chem. Soc. 125 (2003) 9310.
[24] T. Iwamoto, D. Yin, C. Kabuto, M. Kira, J. Am. Chem. Soc. 123 (2001) 12730.
[25] S. Ishida, T. Iwamoto, D. Yin, C. Kabuto, M. Kira, Nature 421 (2003) 725.
[26] A. Sekiguchi, R. Kinjo, M. Ichinohe, Science 305 (2004) 1755.
[27] Z. Pappoport, Y. Apeloig (Eds.), The Chemistry of Silicon Compounds, vol. 2, Wiley, New York, 1998, pp. 1–120.
[28] M.Z. Kassaee, M.R. Nimlos, K.E. Downie, E.E. Waali, Tetrahedron 41 (1985) 1579.
[29] M.Z. Kassaee, B.N. Haerizade, S. Arshadi, J. Mol. Struct. (Theochem) 639 (2003) 187.
[30] M.Z. Kassaee, S.Z. Sayyed-Alangi, Z. Hossaini, J. Mol. Struct. (Theochem) 676 (2004) 7.
[31] M.Z. Kassaee, B.N. Haerizade, Z. Hossaini, J. Mol. Struct. (Theochem) 681 (2004) 129.
[32] M.Z. Kassaee, S.M. Musavi, M. Ghambarian, F. Buazar, J. Mol. Struct. (Theochem) 722 (2005) 151.
[33] M.Z. Kassaee, S.M. Musavi, H. Hamadi, S.E. Hosseini, J. Mol. Struct. (Theochem) 730 (2005) 33.
[34] M.Z. Kassaee, S.M. Musavi, M. Ghambarian, F. Buazar, J. Mol. Struct. (Theochem) 726 (2005) 171.
[35] G. Maier, H.P. Reisenauer, A. Meudt, Eur. J. Org. Chem. (1998) 1313.
[36] A.D. Becke, J. Chem. Phys. 98 (1993) 5648.
[37] J.A. Pople, R. Krishnan, Int. J. Quant. Chem. 14 (1978) 91.
[38] R. Krishnan, M.J. Frisch, J.A. Pople, J. Chem. Phys. 72 (1980) 4244.
[39] J.A. Pople, M. Head-Gordon, K. Raghavachari, J. Chem. Phys. 87 (1987) 5968.
[40] G.E. Scuseria, H.F. Schaefer III, J. Chem. Phys. 90 (1989) 3700.
[41] J.E. Carpenter, F. Weinhold, J. Mol. Struct. (Theochem) 41 (1988) 169.
[42] R.F. Hout, B.A. Levi, W.J. Heher, J. Comput. Chem. 82 (1985) 234.
[43] D.J. Defrees, A.D. McLean, J. Chem. Phys. 82 (1985) 333.
[44] M.J. Frisch, G.W. Trucks, H.B. Schlegel, G.E. Scuseria, M.A. Robb, J.R. Cheeseman, V.G. Zakrzewski Jr., J.A. Montgomery, R.E. Stratmann, J.C. Burant, S. Dapprich, J.M. Millan, A.D. Daniels, K.N. Kudin, M.C. Strain, O. Farkas, J. Tomasi, V. Barone, M. Cossi, R. Cammi, B. Mennucci, C. Pomelly, C. Adamo, S. Clifford, J. Ochterski, G.A. Petersson, P.Y. Ayala, Q. Cui, K. Morokuma, D.K. Malick, A.D. Rabuck, K. Raghavachari, J.B. Foresman, J. Cioslowski, J.V. Ortiz, A.G. Baboul, B.B. Stefanov, G. Liu, A. Liashenko, P. Piskorz, I. Komaromi, R. Gomperts, R.L. Martin, D.J. Fox, T. Keith, M.A. Al-Laham, C.Y. Peng, A. Nanayakkara, C. Gonzalez, M. Challacombe, P.M.W. Gill, B. Johnson, W. Chen, M.W. Wong, J.L. Andres, C. Gonzalez, M.H. Gordon, E.S. Replogle, J.A. Pople, GAUSSIAN 98 package, Gaussian Inc., Pittsburgh, PA, 1998.
[45] B.A. Smith, C.J. Cramer, J. Am. Chem. Soc. 118 (1996) 5490.
[46] K. Aoki, S. Ikuta, A. Murakami, J. Mol. Struct. (Theochem) 365 (1996) 103.
[47] C. Barrientos, A. Cimas, A. Largo, J. Phys. Chem. A 105 (2001) 6724.
[48] P.P. Gaspar, M. Xiao, D. Ho Pae, D.J. Berger, T. Haile, T. Chen, D. Lei, W.R. Winchester, P. Jiang, J. Organomet. Chem. 646 (2002) 68.
[49] G.W. Schriver, M.J. Fink, M.S. Gordon, Organometalics 6 (1987) 1977.